Carbohydrate Polymers xxx (2012) xxx–xxx

Contents lists available at SciVerse ScienceDirect

Carbohydrate Polymers

journal homepage: www.elsevier.com/locate/carbpol

Green synthesis of hyaluronan fibers with silver nanoparticles

A.M. Abdel-Mohsen*, Radim Hrdina, Ladislav Burgert, Gabriela Krylová, Rasha M. Abdel-Rahman, Anna Krejčová, Miloš Steinhart, Ludvík Beneš

Faculty of Chemical Technology, University of Pardubice, Studentská 95, 53210 Pardubice, Czech Republic

ARTICLE INFO

Article history:
Received 23 January 2012
Received in revised form 28 February 2012
Accepted 7 March 2012
Available online xxx

Keywords:
Green chemistry
Hyaluronan fiber
Silver nanoparticles

ABSTRACT

The application of green chemistry in the nano-science and technology is very important in the area of the preparation of various materials. In this work, an eco-friendly chemical method was successfully used for the preparation of hyaluronan fibers containing silver nanoparticles (AgNPs).

Thus, hyaluronic acid (HA) was dissolved in an aqueous solution of sodium hydroxide to prepare a transparent solution, which was used for the preparation of fibers by a wet-spinning technique. Consequently, silver nanoparticles inside the fiber were prepared. Different parameters affecting the preparation of final product, such as concentration of silver nitrate, hyaluronan fiber concentration, time and temperature of the reaction, pH of the reaction mixture, were studied. AgNPs were confirmed by transmission electron microscopy (TEM), X-ray diffraction (XRD), two-dimensional X-ray scattering (2D SWAXS), UV/Vis spectroscopy, inductively coupled plasma optical emission spectrometry (ICP OES) and scan electron microscopy (SEM). Mechanical properties of prepared fibers were also measured.

1. Introduction

Nanostructure noble metal materials have wide-ranging implications in the fields of photonics (Chang, You Apiwat, & Vincent, 2007), catalysis (Steffan, Steffan, Jakob, & Lang, 2009), microelectronics (Sun, Yin, Mayers, Herricks, & Xia, 2002), biosensing (Chen et al., 2007) and antimicrobial functionalities (Du, Du, Niu, Xu, & Fan, 2009), etc. Among these, the use of nanosized silver particles (AgNPs) as a substrate for enhancing the surface, plasmon resonance has been widely reported (Nogueira, Soares, Cruz, & Trindade, 2002), in which the well defined shape and structure of Ag nanoparticles are critical to the optimum enhancement. In the past decades, many effective methods have been developed for the synthesis of Ag nanoparticles (Hideki, Kanda, Shibata, Ohkubo, & Abe, 2006; Pastoriza & Liz, 1999; Van, Klemperer, Wo, & Zukoski, 2001). However, the environmental and biological risks are usually caused due to the use of noxious reducing and/or stabilizing agents in the synthesis procedures, like sodium borohydride [9], hydrazine (Nogueira, Soares, Cruz, & Trindade, 2002) and *N,N*-dimethyl formamide (Lapcik, Smedt, Demeester, & Chabrecek, 1998). With the increasing awareness of environmental protection, people are inclined to focus on the green chemistry. For this purpose, the natural compounds like D-glucose (Raveendran, Fu, & Wallen, 2003) and chitosan (Abdel-Mohsen et al., 2012; Dash, Chiellini, Ottenbrite, & Chiellini, 2011; Muzzarelli, 2011; Wan, Sun, Li, & Li, 2009) was used to stabilize the Ag nanoparticles with other reducing agents. In addition, the soluble starch has been used as both the reducing and stabilizing agents to synthesize the Ag nanospheres via a one-pot green method (Vigneshwaran, Nachane, Balasubramanya, & Varadarajan, 2006). Green synthesis of Ag-NPs involve three main steps, which must be evaluated based on green chemistry perspectives, including selection of solvent medium, reducing agent, and non toxic substance for AgNPs stability (Raveendran, Fu, & Wallen, 2006).

Hyaluronic acid (HA) is natural polysaccharide with a repeat unit of D-glucuronic acid and *N*-acetylglycosamine (Scheme 1), existing in many connective tissues of mammals such as cartilage, the central component for structuring the tissue (Lubomir, Stefan, Joseph, & Peter, 1998), and it is a green chemical. It is also used as a diagnostic indicator for many diseases such as tumor and liver diseases (Eriksson, Fraser, Laurent, Pertoft, & Smedsrod, 1983). Thus, it is of great importance to study or detect hyaluronic acid in a biological system. Recently Raman spectroscopy has been employed to investigate the structure of hyaluronic acid (Alkrad, Mrestani, Stroehl, Wartewig, & Neubert, 2003; Reineck, DeAnna, Suleski, Lee, & Rupprecht, 2003). However, it has only been used to detect and characterize a bulk HA film. It is known that Ag nanostructure plays a critical rule in SERS (Kvitek et al., 2005; Nogueira, Soares, Cruz, & Trindade, 2002; Tao et al., 2003) for sensitive Raman detection. Hyaluronic acid abundant hydroxyl groups in D-glucuronic acid units have reductive properties (Kvitek et al., 2005; Gao et al., 2005).

In a neutral solution, HA posses negatively charged carboxyl groups, which can electrostatically interact with Ag^+ ions to form

* Corresponding author. Tel.: +420 773063837; fax: +420 466038004.
E-mail address: abdo_mohsennrc@yahoo.com (A.M. Abdel-Mohsen).

0144-8617/$ – see front matter © 2012 Elsevier Ltd. All rights reserved.
doi:10.1016/j.carbpol.2012.03.022

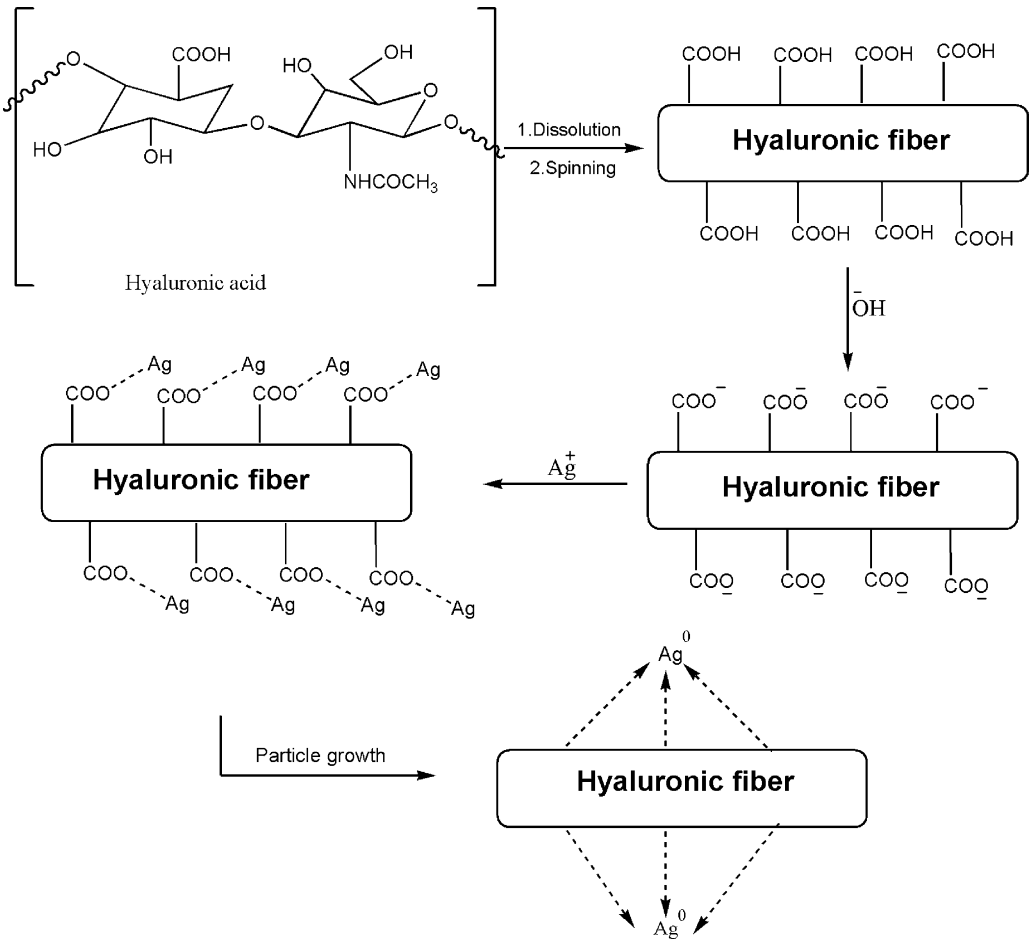

Scheme 1. Preparation of hyaluronan fiber with silver nanoparticles.

a complex as the part of Ag nanostructure. Three main steps in the preparation of nanoparticles that should be evaluated from a green chemistry perspective are the choice of the solvent medium used for the synthesis, the choice of an environmentally benign reducing agent, and the choice of a nontoxic material for the stabilization of the nanoparticles. Most of the synthetic methods reported to date rely heavily on organic solvents. This is mainly due to the hydrophobicity of the capping agents used. There have been approaches reported (Templeton, Chen, Cross, & Murray, 1999) for the synthesis of water-soluble metal nanoparticles. However, to date a unified green chemistry approach to the overall process of nanoparticle production has not been reported.

In the present approach, methanol was utilized as the environmentally benign solvent throughout the preparation. The second concern in a green nanoparticle preparation method is the choice of the reducing agent. The majority of methods reported to date use reducing agents for preparation of AgNPs. The use of a strong reducing agent, such as $NaBH_4$, results in tiny particles that are well-dispersed (Ji, Chen, Wai, & Fulton, 1999; Shah, Holmes, Doty, Johnston, & Korgel, 2000). Nowadays, a succession of chemical reductants used for synthesis of noble metal nanoparticles which contain $NaBH_4$ (Shameli, Ahmad, & Yunus, 2010; Shen, Shi, & Li, 2010), NH_2OH (Wu, Chen, & Huang, 2001), N_2H_2 (Mayer, Grebner, & Wannemacher, 2000; Underhillm & Liu, 2000), $(CH_3)_2NH{\cdot}BH_3$ (Torigoe, Suzuki, & Esumi, 2001), H_2 (Henglein & Giersig, 2000), formaldehyde (Mayer, Grebner, & Wannemacher, 2000), formamide (Han, Quek, & Huang, 1999), Tollens reagents (Yin, Li, & Zhong, 2002), ethylene glycol (Wang, Ren, & Deng, 2000), ethanol (Wang et al., 2000), citrate (Pathak, Greci, & Kwong, 2000), aniline (Tan, Li, & Zhu, 2003), polyaniline (Wang, Neoh, & Kang, 2001), or ascorbic acid (Lim, Jiang, & Yu, 2010). The final and perhaps most important issue in the preparation of nanoparticles is the choice of the capping material used to protect or passivity the nanoparticle surface. There are several issues that should guide the choice of the capping agent, and these vary significantly from the required size ranges and morphologies of the nanoparticles to the targeted application.

In the presented preparation method, a hyaluronic fiber (or better a hyaluronan molecule) serves as the protecting and stabilizing agent. Thus, in this work the hyaluronan fiber was prepared and used it as the reductive and stabilizing agent to prepare the Ag nanoparticles, where the effect of reaction conditions, including the pH value, temperature, concentration of silver nitrate, time and molar ratio of HA to $AgNO_3$ on the size and morphology of AgNPs are discussed. Furthermore, silver nanoparticles incorporated in hyaluronic acid fiber were confirmed by transmission electron microscopy (TEM), two-dimensional X-ray scattering (2D SWAXS) X-ray diffraction, UV/Vis spectroscopy, inductively coupled plasma optical emission spectrometry (ICP OES), scan electron microscopy (SEM). The mechanical properties of prepared HA-AgNPs fibers were also measured.

2. Experimental

2.1. Materials

Sodium hyaluronate high molecular weight (1.75 MDa, determined by SEC-MAALS) was purchased from CPN Ltd.,

Please cite this article in press as: Abdel-Mohsen, A. M., et al. Green synthesis of hyaluronan fibers with silver nanoparticles. *Carbohydrate Polymers* (2012), doi:10.1016/j.carbpol.2012.03.022

Dolni-Dobrouč, Czech Republic, sodium hydroxide, formic acid, acetic acid, silver nitrate, and methanol were obtained from Sigma–Aldrich, Germany. Deionized water was used for all experiments.

2.2. Methods

2.2.1. Preparation of hyaluronan fibers

Sodium hyaluronate (1.75 MDa, 6 g) was dissolved under stirring in 94 g of water with the addition of NaOH (0.64 g) to obtain homogenous, well-flowing viscous solution suitable for spinning. This solution was pressed (wet-spinning technique) trough a nozzle with the diameter of 0.4 mm to the coagulation bath having the composition: 600 ml of methanol and 400 ml of acetic acid (98%). The prepared fibers were left in the coagulation bath for 15 h, then washed with absolute methanol and dried.

2.2.2. Preparation of silver nanoparticles incorporated in hyaluronic fibers

Silver nanoparticles were prepared by means of a simple chemical reduction of silver nitrate by hyaluronic fibers, respectively by hyaluronan. A certain weight of the so-prepared (HA fiber) was dispersed in a certain volume of methanol using a heating magnetic stirrer. After dispersion of HA in methanol, the pH of the solution was adjusted within the range (4–11.5), followed by the raising of temperature (20–80 °C). A certain amount of silver nitrate solution was then added drop-wise. The reaction mixture was kept under continuous stirring for different time (15–180 min). Short time after the addition of silver nitrate, the HA fiber acquires a clear yellow color indicating the formation of silver nanoparticles. The progression of the reaction was controlled by UV/Vis absorption; aliquots from the reaction bulky were withdrawn at given time intervals and evaluated.

2.3. Characterization of silver nanoparticles incorporated hyaluronic fibers

2.3.1. Inductively coupled plasma optical emission spectrometry (ICP OES)

The elemental analysis of silver was carried out with the sequential, radially viewed inductively coupled plasma atomic emission spectrometer INTEGRA XL 2 (GBC, Dandenong Australia), equipped with the ceramic V-groove nebulizers and the glass cyclonic spray chamber (both Glass expansion, Australia). For an instrumental calibration (1–0.5–0.1–0.05–0.02 mg l^{-1}), a commercially available stock standard solutions of Ag containing 1 g L^{-1} (SCP, Baie Duffer, Canada) were used. The limits of detection (the concentration equivalent to three times standard deviation of the blank sample in the place of background correction) were 10 μg l^{-1} for lines 338.289 nm and 328.068 nm. For analysis of real samples, results from both analytical lines used were averaged.

2.3.2. Scan electron microscopy (SEM)

The images of samples were done at the electron-scanning microscope at the CPN Ltd., Tuscan VEGA II LSU electron microscope (Tuscan USA Inc.) under the following conditions: high voltage 5 kV, working distance 4.4 mm, display mode secondary electrons, high vacuum, room temperature. SC7620 Mini Sputter Coater (Quorum Technologies, UK) applied 15 nm layers of gold particles on the sample. The samples were dusted for 120 s with the current of 18 mA. The pictures were made at these conditions: voltage 2.44–10 kV, detector: SE. the magnification 300–20,000 times, vacuum high, the distance between sample and objective: 4–5 mm.

2.3.3. UV–visible spectroscopy

Measurements were carried out on UV-visible spectrophotometer UV-160A (Shimadzu, Japan) using quartz cuvettes with an optical path of 1 cm. The concentration of the measured solutions was kept at 0.59 mg/ml.

2.3.4. Transmission electron microscopy (TEM)

TEM images were observed on a JEOL JEM-2010 (HT) electron microscope, using an accelerating voltage of 200 kV. The samples were dissolved in deionized water or aqueous alkaline solution with concentrations of 0.5 mg/ml, and a drop was placed on Cu grids precoated with carbon films.

2.3.5. X-ray diffraction (XRD)

Powder X-ray diffraction data (Cu Kα, $\lambda = 1.5418$ Å) were collected on a D8 Advance diffractometer (Bruker AXS, Germany) with Bragg–Brentano θ–θ goniometer (radius 217.5 mm) equipped with a secondary beam curved graphite monochromator and Na(Tl)I scintillation detector. The generator was operated at 40 kV and 30 mA. The scan was performed at room temperature from 2 to 70° (2θ) in 0.02° step with a counting time of 8 s per step.

2.3.6. Two-dimensional X-ray scattering (2D SWAXS)

SAXS and WAXS experiments were performed using a 3 pinhole camera (Molecular Metrology SAXS System now Rigaku) attached to a multilayer aspherical optics (Osmic Confocal Max-Flux) which at the same time monochromatises as well as focuses the beam of a microfocus X-ray tube (Bede microsource) operating at 45 kV and 0.66 mA (30 W). SAXS patterns were measured by means of a multi-wire, gas-filled area detector with an active area diameter of 20 cm (Gabriel design). WAXS diffractograms were measured using an image plate. Calibration was done using Silver Behenate in SAXS and Si powder in WAXS region. Peak positions were employed to obtain characteristic length D according to Bragg's law, $d = 2\pi/q$, where $q = (4\pi/\lambda)\sin(\theta)$, where $\lambda = 0.154$ nm is the wavelength, same as in the powder diffraction measurements and 2υ is the scattering angle. Measurements were optimized to reach reasonable counting statistics and usually took from 4 to 10 h.

3. Results and discussion

3.1. Preparation of hyaluronan fibers

Hyaluronan fibers were prepared by wet-spinning technique described in the literature (Burgert et al., 2010). Hyaluronic acid was dissolved in slightly alkali water solution of sodium hydroxide, after dissolution completely of hyaluronic acid to obtain transparent solution (5.96 mass% of HA). In this system, water and sodium hydroxide are nontoxic and inexpensive. It should be noted that there was no evaporation of any chemical agents during dissolution of hyaluronic acid at room temperature, thus clean air and environment was maintained during the production of HA fibers. The byproduct in the coagulation bath is mainly sodium acetate, which can by separated and evaporated easily. Therefore, this bath procedure is a real green technology, because it is nonpolluting, and it is easy to recycle its byproduct. Furthermore, there is no evaporation of the chemical agents during the process. The solution of hyaluronic acid solution was used for wet spinning, where the nozzle had the diameter 0.4 mm. As the coagulation bath, the mixture of 600 ml of methanol and 400 ml of acetic acid was used; homogenous fibers were obtained. The prepared fibers were left in the coagulation bath for 15 h, then washed with absolute methanol and dried.

Please cite this article in press as: Abdel-Mohsen, A. M., et al. Green synthesis of hyaluronan fibers with silver nanoparticles. *Carbohydrate Polymers* (2012), doi:10.1016/j.carbpol.2012.03.022

3.2. Formation of silver nanoparticles inside of HA-fiber

Hyaluronan fibers played a dual role: as a reducing agent for silver ions and as a stabilizing agent during/after the formation of silver nanoparticles. Factors affecting the reduction efficiency and stability as well as the shape and the size of the formed silver nanoparticles along with mechanisms involved are given below.

The silver ions interact with the available functional groups of hyaluronic acid fibers. Hyaluronic acid is known to be rich by different functional groups such as hydroxyl, carboxyl, and acetamide groups. All these groups work as powerful "reduction and stabilizing agents" to prepare silver nanoparticles (Abdel-Mohsen et al., 2012). Further, these nanoparticles are probably capped and stabilized by a polysaccharide matrix. The structure of hyaluronic acid is very complex; it is most likely that more than one mechanism is involved in the reaction of silver ion with hyaluronic fiber and subsequent reduction of silver ions (as it is shown in Scheme 1). Silver ions complication by hydroxyl and acetamide groups and its subsequent stabilizing by carboxyl groups.

3.2.1. Effect of pH of reaction medium

Hyaluronic acid fiber plays a dual role during the preparation of nano-sized silver nanoparticles. The first one is to generate complex compound with silver ions and control the reduction process. The second role is to protect the particles from aggregation and accumulation.

Thus, 0.1 g of hyaluronic fiber (unit $C_{14}H_{21}NO_{11}$, 0.26 mM) was dispersed in 24 ml of methanol using a heating magnetic stirrer. After dispersion of hyaluronic fibers, the pH was adjusted to 4, 6, 9, and 11.5 using dilute acetic acid (1 M) and sodium hydroxide solutions (IM) while the temperature raised to 60 °C. At the end, silver nitrate was added drop wise (700 μl, 10 mM), keeping in mind that the total volume of the reaction medium is 25 ml. The reaction was allowed to proceed under continues stirring for 1 h where by AgNPs was formed.

Fig. 1A shows the UV/Vis spectra of silver nanoparticles obtained using hyaluronic fiber as the reducing and stabilizing agent at different pH. The results reveal a number of observations which may be summarized as follows: (a) increasing the pH of the reaction medium is accompanied by appreciable changes in the electronic absorption spectra; (b) the band at higher energy (360 nm) appears at pH 4; the intensity of this band decreases by the increasing of pH up to 9; an further increase in the pH of reaction medium up to 9 leads to disappearance of this band; (c) simultaneously another band at 408 nm starts to appear and reaches its maximum intensities at pH 11.5 and when the range of pH is targeted, the band becomes stronger and symmetrical, with a pronounced bell shape at λ_{max} (408 nm). This band could be assigned to the plasmon resonance of silver nanoparticles.

In the right side in Fig. 1A, the photograph of dissolved hyaluronic fibers in water is presented, where the change of color from colorless (pure hyaluronan fiber) in the left to yellowish (silver nanoparticles) in the relation to the pH of reaction medium can be seen.

The pH value is usually the key factor in the preparation of silver nanoparticles especially in the reduction step. When the pH value is near to the isoelectric point (about 3), a hyaluronic fiber possess uncharged carboxyl groups leading the molecular chains to shrink to a coiled state. When the pH value is higher than 4, the carboxyl groups will be negatively charged due to their hydrolysis. In our opinion, this ionization converts a double helical structure of hyaluronic acid to a linear conformation similarly to (Sheng, Yangyang, xiaojuan, & Lina, 2011). So that, the higher pH value of reaction medium would lead to more exposed carboxyl groups electrostatically interacting with Ag^+ by HA, and promote its reduction, in which the experiments were preformed at 60 °C. At pH 4, a band at about 360 nm was observed even after 1 h at 60 °C, which corresponded to the existence of Ag^+ clusters. With the increase of the pH value, a new band appeared at about 408 nm on the UV/Vis spectra of the samples, suggesting the formation of silver nanoparticles.

Fig. 1B shows the percentage of silver nanoparticles incorporated into hyaluronan fibers. It can be seen that the increase of reaction medium pH is increasing the silver percentage. This is due to an increasing of the content of "free carboxylic groups" in a fiber, since their inter and intra hydrogen bonds inside the hyaluronic fiber are interrupted. This means that the increasing of carboxylic groups in anion form will enhance the electrostatic interaction between the negative charge of carboxylic groups on the surface and inside of hyaluronic fibers (COO^-) and the positive charge of silver ions (as shown in Scheme 1).

Fig. 2 shows the transmission electron microscopy (TEM) images and particle size distribution histogram of silver nanoparticles with the preparation pHs. The average size of spherical Ag nanoparticles became smaller by increasing the pH values, which is about 45, 35, 20, 10, and 6 nm in Fig. 2a–e corresponding to 4, 6, 9, 10, and 11.5 of pH value respectively.

3.2.2. Silver nitrate concentrations

In this part of our work, we were focused on the relationship between the concentration of $AgNO_3$ in the preparative reaction mixture and resulted Ag^0 nanoparticles.

Fig. 3A shows the UV/Vis spectra of Ag^0 resulting from incorporating different amount of silver nitrate (0.1–15 mM). As can be found, the absorption peak at approximately 410 nm is constituent with that silver nanoparticle. From obtained data, it can be concluded that higher concentration of silver nitrate (0.1–15 mM) leads to the higher numbers of silver nanoparticles (Fig. 3B). This result is mainly attributed to the fact that the rate of spontaneous nucleation increases significantly the growth rate of silver nanoparticles. Large numbers of nuclei was formed during the nucleation burst. However, the particle size doses not become larger owing the presence of hyaluronic fiber macromolecules. Therefore, it is possible that a large amount of silver nanoparticles with small particles size can be achieved.

3.2.3. TEM and histogram of silver nanoparticles prepared at different concentrations of silver nitrate

Fig. 4 shows the TEM micrograph and the corresponding particles size distribution of silver nanoparticles with a different concentration of silver nitrate. Fig. 4a shows TEM of silver nanoparticles with a concentration 0.1 mM of silver nitrate. The reaction was prepared containing 0.1 g of hyaluronic fiber dispersed in 25 ml of methanol. The pH of the reaction medium was adjusted to pH 11.5 and the reaction was allowed to proceed at 60 °C for 1 h keeping in mind the total volume of the reaction is 25 ml. Consequently, Fig. 4b illustrates a histogram showing the particle size distribution of AgNPs at $AgNO_3$ concentration 1 mM (700 μl). Fig. 4c–f shows the TEM of silver nanoparticles with a different concentration of silver nitrate (3, 5, 10, 15 mM) respectively. Histograms showing the particle size distributions of silver nanoparticles. From the obtained results, it can be concluded, that at the concentration of $AgNO_3$ higher than 10 mM (700 μl) an aggregation of particles occurs (Fig. 4f). Therefore, in the respect, that we want to prepare the fibers with well-distributed silver nanoparticles, the most suitable concentration of $AgNO_3$ in the preparation is 10 mM.

3.2.4. Effects of time, temperature, concentration of hyaluronic fiber, and storage time on the synthesis of silver nanoparticles.

The formation of silver nanoparticles inside the fiber could be easily followed through its distinctive color changes, where within few minutes of the reaction the fiber color change became from

Please cite this article in press as: Abdel-Mohsen, A. M., et al. Green synthesis of hyaluronan fibers with silver nanoparticles. *Carbohydrate Polymers* (2012), doi:10.1016/j.carbpol.2012.03.022

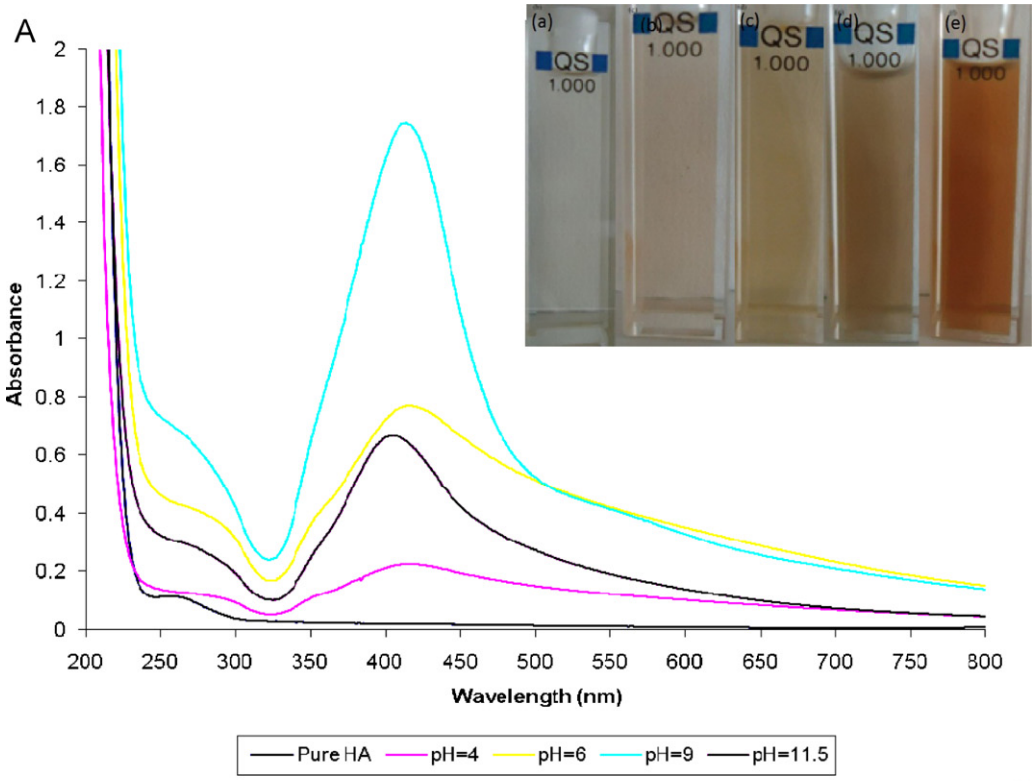

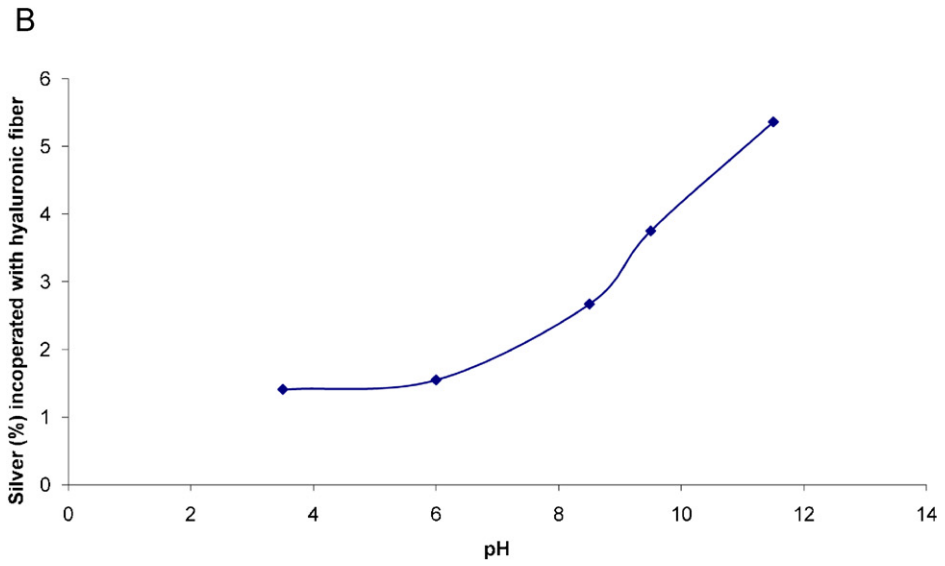

Fig. 1. (A) UV/Vis spectroscopy of silver nanoparticles prepared at different pH. The photograph in right side (A) changing of the sample color during the change the pHs of reaction medium. (B) Concentration of silver inside of HA-Ag fibers prepared at different pH. *Experimental conditions*: hyaluronic fiber (0.1 g, 0.26 mM); 25 ml of methanol; 700 μl of $AgNO_3$ (10 mM), temperature, 60 °C; reaction time 60 min.

pale yellowish to pale red. The effect of the reaction time on prepared silver nanoparticles is summarized in Fig. 5A. After 15 min of reaction, a slight absorption band at 405 nm appeared which became clearly visible at 45 min suggesting the presence of spherical silver nanoparticle in the system (Jradi et al., 2010). However, further increase of reaction time is increasing the absorption peak (405 nm) intensity significantly and some "red enlargement" of this peak appeared, both facts suggesting the increasing number of nanoparticles (Bohren & Huffman, 1998).

Fig. 5B shows the effect of reaction temperature on the $Ag^+ \rightarrow Ag^0$ reduction where the experiments were performed under the reaction conditions: the volume of silver nitrate 700 μl (10 mM), pH 11.5. It is known that the absorption band appears at 405–433 nm because the surface plasmon resonance. The data indicate that at 40–50 °C the reduction efficiency is not enough for the complete transformation of Ag^+ into silver nanoparticles (weak peaks characteristic for Ag^+ are found at the wavelength 270 nm). The increase of the reaction temperature above 60–75 °C leads to disappearance of the peak characteristic for Ag^+, indicating its complete transformation to Ag^0.

Fig. 5C shows the UV/Vis absorption spectra of silver nanoparticles prepared by the use of hyaluronic fibers in different

Please cite this article in press as: Abdel-Mohsen, A. M., et al. Green synthesis of hyaluronan fibers with silver nanoparticles. *Carbohydrate Polymers* (2012), doi:10.1016/j.carbpol.2012.03.022

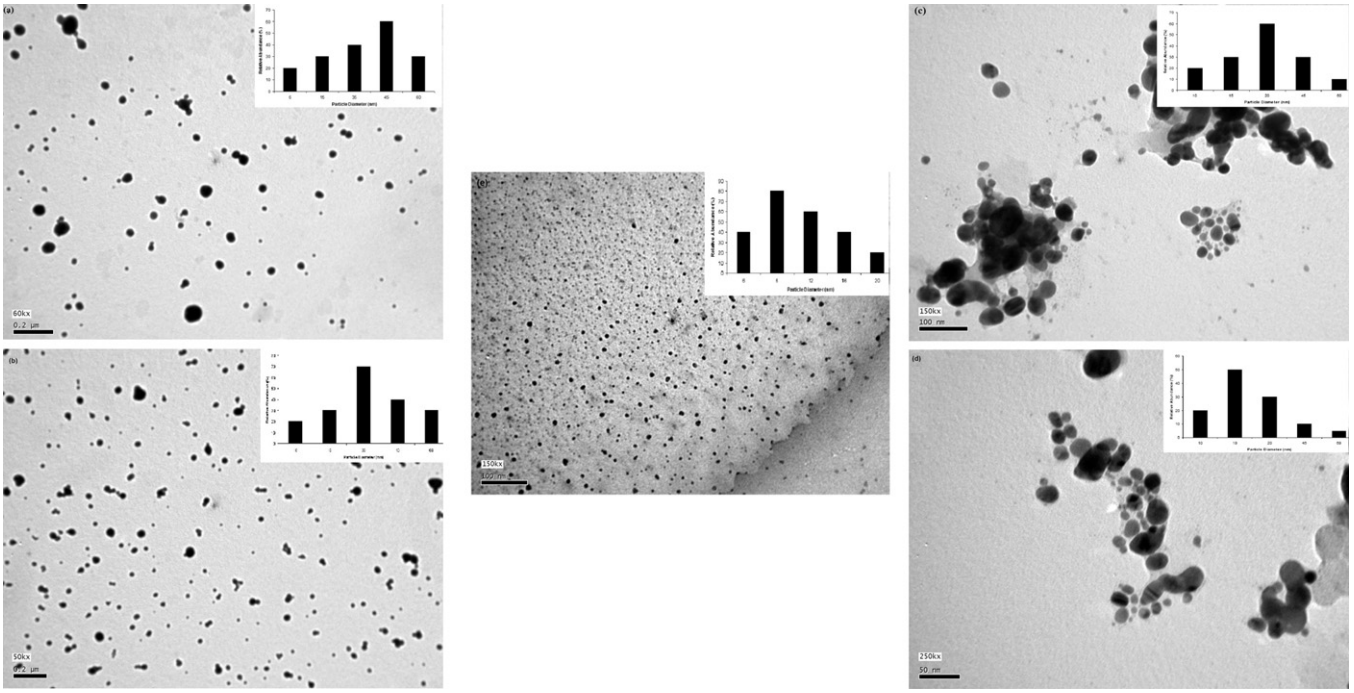

Fig. 2. Transmission electron microscopy images and their particle size distributions of silver nanoparticles upon hyaluronic acid on the pHs of preparation medium (a), pH 4; (b) pH 6; (c) pH 9; (d) pH 10; and (e) pH 11.5. *Experimental conditions*: hyaluronic fiber (0.1 g, 0.26 mM); 700 μl of $AgNO_3$ (10 mM), temperature, 60 °C; reaction time 60 min.

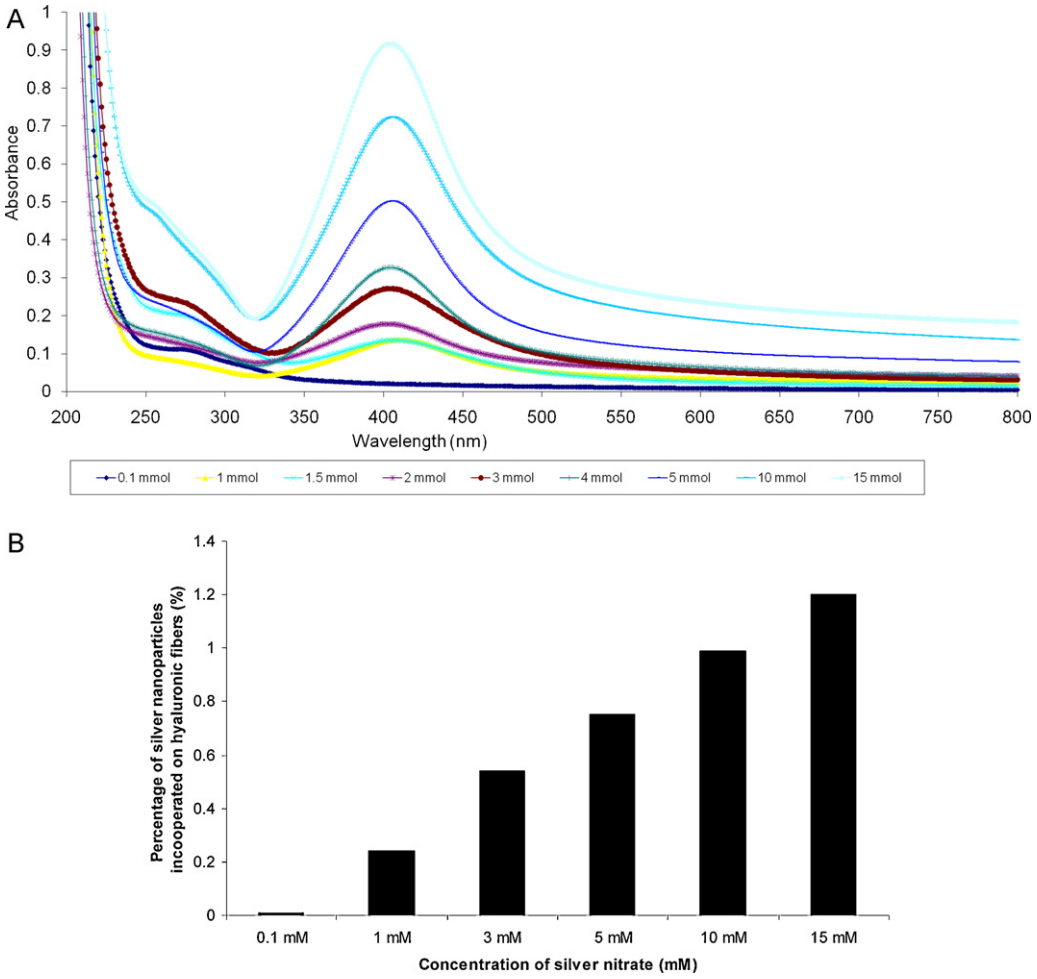

Fig. 3. (A) UV/Vis spectroscopy of silver nanoparticles prepared by different concentration of silver nitrate. (B) Percent of silver nanoparticles incorporated in HA-Ag fiber. *Experimental conditions*: hyaluronic fiber (0.1 g, 0.26 mM); temperature 60 °C; reaction time 60 min; 25 ml methanol; pH 11.5.

Please cite this article in press as: Abdel-Mohsen, A. M., et al. Green synthesis of hyaluronan fibers with silver nanoparticles. *Carbohydrate Polymers* (2012), doi:10.1016/j.carbpol.2012.03.022

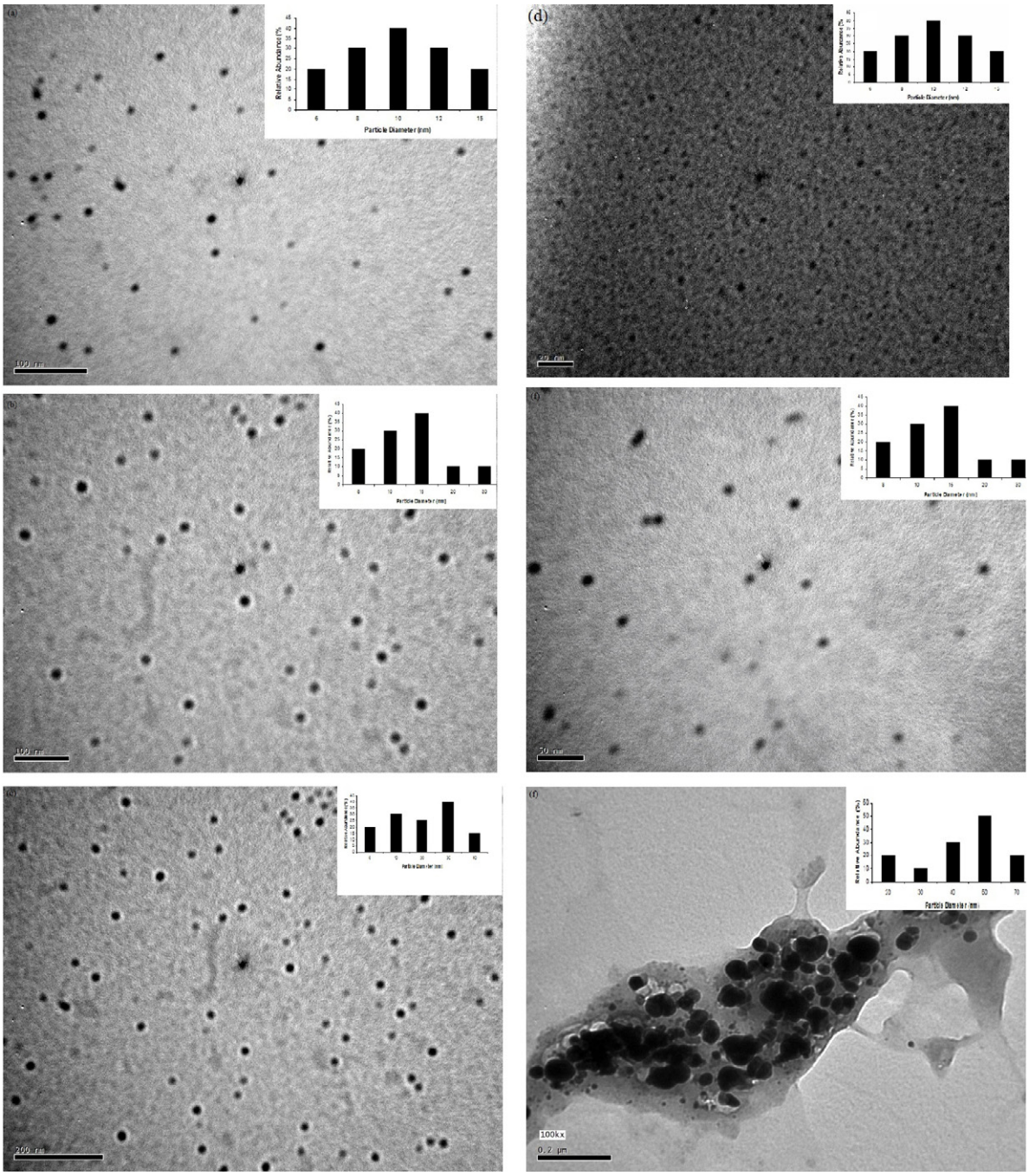

Fig. 4. TEM images and histogram showing the corresponding particle size and particle size distribution of silver nanoparticles at different concentrations of silver nitrate; (A) 0.1 mM; (b) 1 mM; (c) 3 mM; (d) 5 mM; (e) 10 mM; and (f) 15 mM. *Experimental conditions*: hyaluronic fiber (0.1 g, 0.26 mM); temperature 60 °C; reaction time 60 min; 25 ml methanol; pH 11.5.

concentrations (0.025–2%) at the fixed concentration of silver nitrate (700 μl, 10 mM) and at pH 11. The data reveal that regardless of used hyaluronic fibers, similar plasmon bands are formed at wavelengths ~405–410 nm with the bell shape. This phenomenon is characteristic for formation of Ag^0 nanoparticles. It is also clear that there is a gradual increase in the absorption intensity, by increasing the hyaluronic fibers up to 2%, which could be ascribed to the enhancement in the stabilization efficiency of the formed silver nanoparticles. It should be also mentioned even the least amount of HA fibers in the reaction medium (0.4%) is enough for the full reduction of Ag^+ to Ag^0. The aforementioned study concluded the optimal conditions for the production of hyaluronic fibers incorporated by silver nanoparticles.

Therefore, an optimal sample was made at room temperature (Fig. 5D), then it was stored in a dark room for the evaluation of stability. Thus, the stability of prepared sample was evaluated within 3 months. The stability of AgNPs during the storage time was traced at different aging periods by the UV/Vis spectroscopy for samples diluted/dissolved 10 times with de-mineralized water. As can be seen from Fig. 5D, the intensity of plasmon absorption band displayed a slight decrease after 90 days. In addition, the maximum of the absorbance peak was nearly the same as the as-prepared sample was 408 nm against 403 nm for the 90 days aged sample. From these results it is believed, that the AgNPs in hyaluronan fibers are very stable against aggregation during several months.

Please cite this article in press as: Abdel-Mohsen, A. M., et al. Green synthesis of hyaluronan fibers with silver nanoparticles. *Carbohydrate Polymers* (2012), doi:10.1016/j.carbpol.2012.03.022

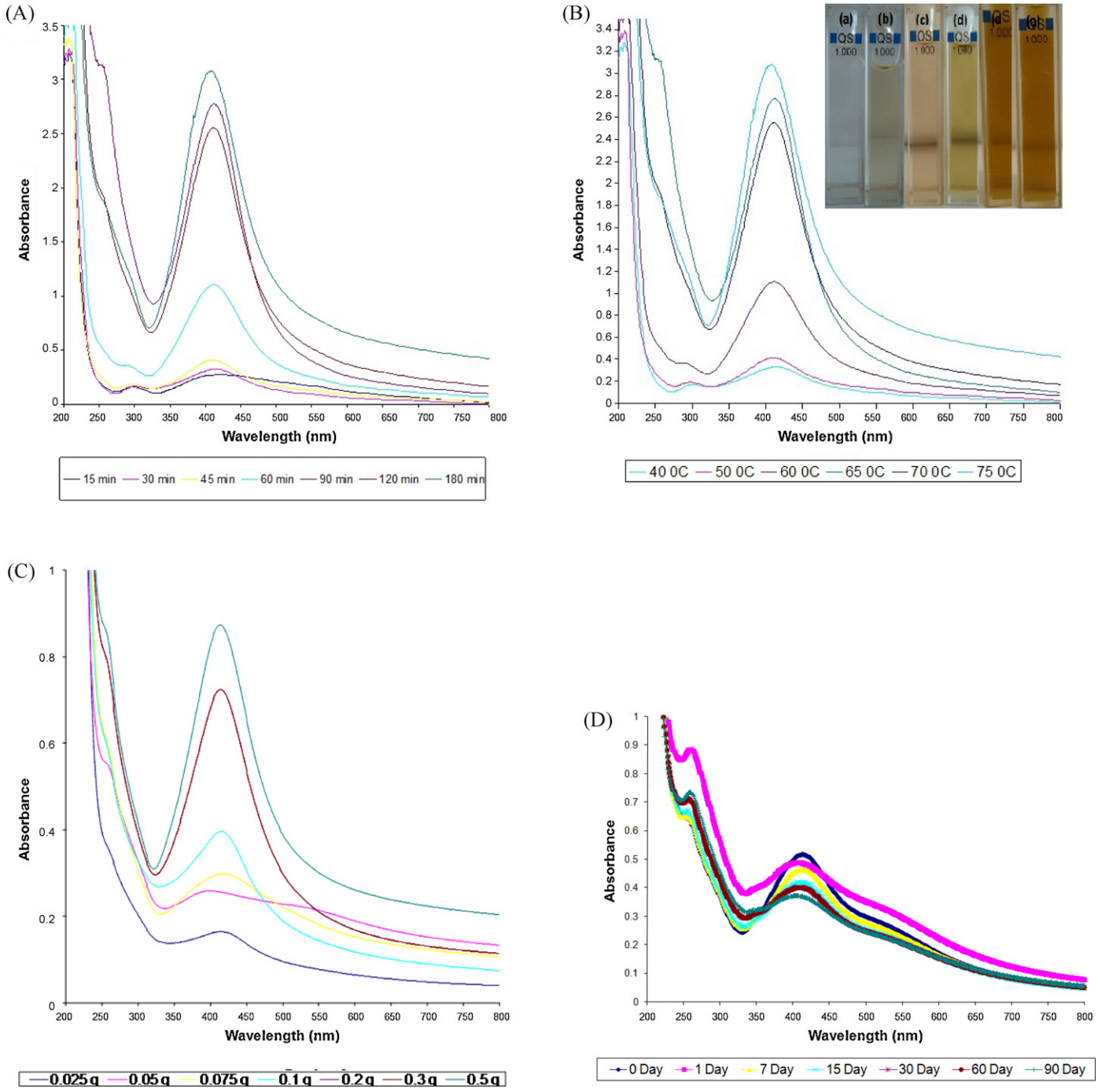

Fig. 5. UV/Vis spectroscopy of Hyaluronan fiber-silver nanoparticles. (A) UV/Vis spectra of silver nanoparticles prepared at different times; (B) UV/Vis spectra of silver nanoparticles prepared at different temperatures; (C) UV/Vis spectra of silver nanoparticles prepared at different concentrations of HA fiber; and (D) effect of storage time on hyaluronan fiber with silver nanoparticles (10 mmol).

3.2.5. Photograph, powder-X-ray diffraction, and SEM of hyaluronan fiber with silver nanoparticles

Fig. 6A shows the photos of pure hyaluronic fiber (colorless) and fibers with silver nanoparticles. To investigate the crystal structure of pure hyaluronic fiber and silver nanoparticles after aging, the samples were further analyzed by powder XRD (Fig. 6B).

The diffraction diagram of pure hyaluronic fiber (Fig. 6B-a) shows only a broad peak with maximum 2θ about 20° related to hyaluronic acid. This broad band is also preserved in the diffractograms of both samples of hyaluronic fibers with silver nanoparticles (Fig. 6B-b and c). The XRD peaks at 2θ = degrees of 38.1, 44.3, 64.5, and 77.5 can be attributed to the (1 1 1), (2 0 0), (2 2 0) and (3 1 1) diffraction lines of face-centered-cubic (fcc) crystalline structure of metallic silver. Diffraction line observed at $2\theta = 30.9°$ (interlayer distance of 2.888 Å) corresponds to interlayer distance of (1 1 0) planes of silver (2.889 Å) but these planes should not diffract in the case of fcc structure. It seems probable that during formation of silver nanoparticles the fcc arrangement of silver was distorted due to some shift of layers of silver atoms, or in a nanoparticles the selection rules are not completely valid.

Fig. 6C shows the SEM photographs of pure hyaluronic fiber and AgNPs in hyaluronic fiber. Fig. 6C-a shows the pure hyaluronic fiber

Please cite this article in press as: Abdel-Mohsen, A. M., et al. Green synthesis of hyaluronan fibers with silver nanoparticles. *Carbohydrate Polymers* (2012), doi:10.1016/j.carbpol.2012.03.022

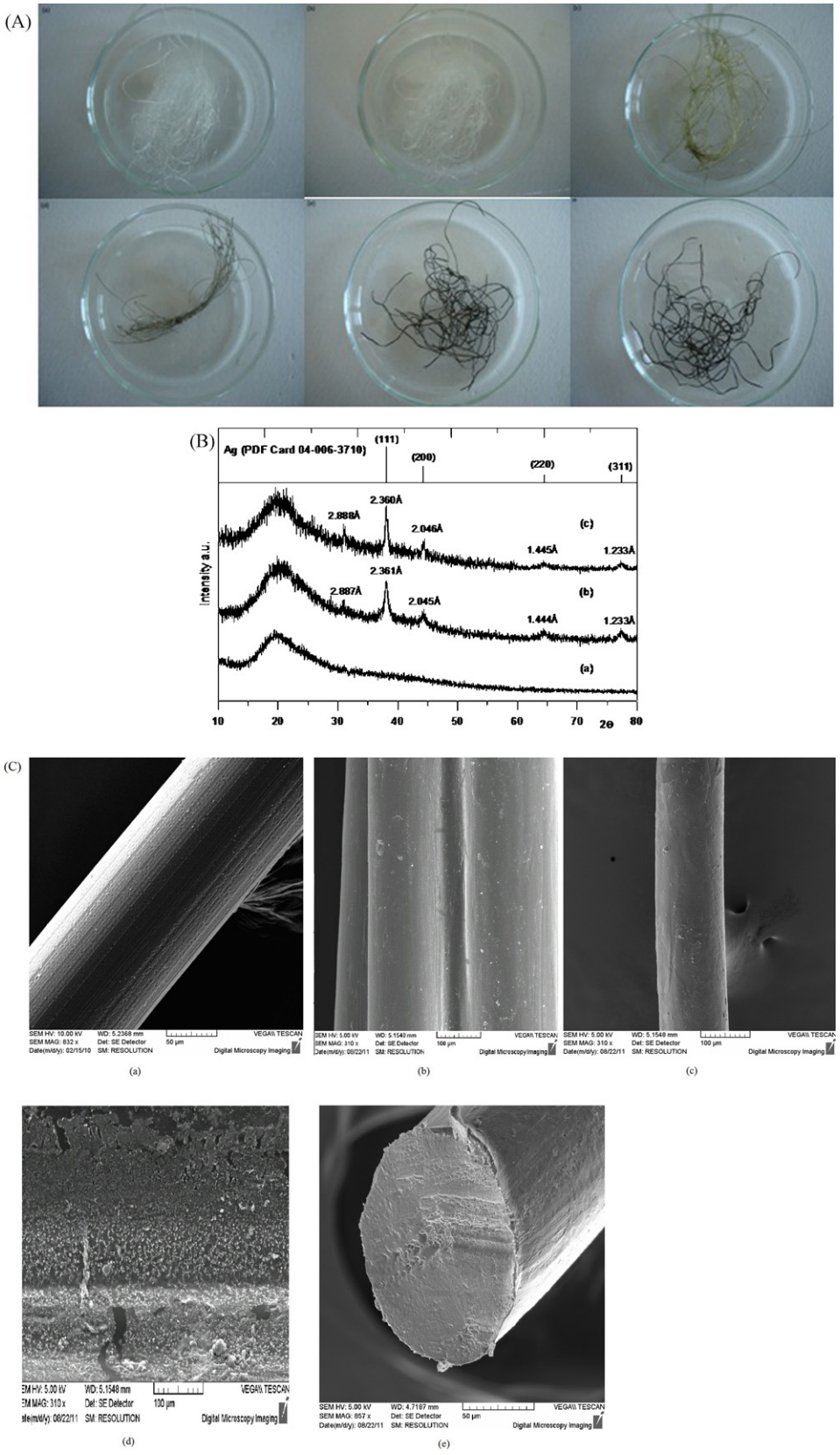

Fig. 6. Photograph, XRD, and SEM of hyaluronan fibers with silver nanoparticles. (A) Photos of hyaluronic fibers with silver nanoparticles. (a) Hyaluronic fiber pure; (b) hyaluronic fiber with silver nanoparticles (0.1 mmol); (c) hyaluronic fiber with silver nanoparticles (0.5 mmol); (d) hyaluronic fiber with silver nanoparticles (1 mmol); (e) hyaluronic fiber with silver nanoparticles (5 mmol); and (f) hyaluronic fiber with silver nanoparticles (10 mmol). (B) XRD of hyaluronic fibers with silver nanoparticles. (a) Pure hyaluronic fiber; (b) hyaluronic fibers with silver nanoparticles (5 mM); and (c) hyaluronic fibers with silver nanoparticles (10 mM). (C) SEM of hyaluronic fibers with silver nanoparticles. (a) Pure hyaluronic fiber; (b) hyaluronic fiber with silver nitrate (1 mM); (c) hyaluronic fibers with silver nanoparticles (5 mM); (d) hyaluronic fibers with silver nanoparticle (10 mM); and (e) cross-section of silver nanoparticle incorporated with Hyaluronic fibers (10 mM).

Please cite this article in press as: Abdel-Mohsen, A. M., et al. Green synthesis of hyaluronan fibers with silver nanoparticles. *Carbohydrate Polymers* (2012), doi:10.1016/j.carbpol.2012.03.022

Table 1
Effect of concentration of silver nitrate on the mechanical properties of hyaluronan fiber.

Concentration of silver nitrate	Genteelness (tex)	Load at break (N)	Tensile strain (mm/mm)	Modulus Young's (gf/tex)	Strength (GPa)	Relative strength (Mn/dtex)
Pure hyaluronan fiber	73.14	4.23	0.11	122.21	0.65	3.37
0.1 mM	94.07	2.9	0.07	81.95	0.41	1.83
0.5 mM	67.81	3.91	0.09	120.25	0.68	3.39
1 mM	64.51	3.58	0.1	123.43	1.47	3.17
1.5 mM	76.52	3.09	0.06	97.99	0.88	2.32
2 mM	74.28	1.86	0.04	63.52	0.51	1.47
3 mM	55.18	3.63	0.08	231.78	1.13	3.68
4 mM	52.61	3.09	0.04	224.25	0.56	3.34
5 mM	44.34	2.52	0.04	175.03	0.89	3.33
10 mM	62.88	4.04	0.09	230.31	1.41	4.48

Reaction conditions: hyaluronan fiber (0.1 g, 0.26 mM); volume of methanol, 25 ml; hydroxide; pH, 11.5; duration time, 60 min; reaction temperature, 60 °C.

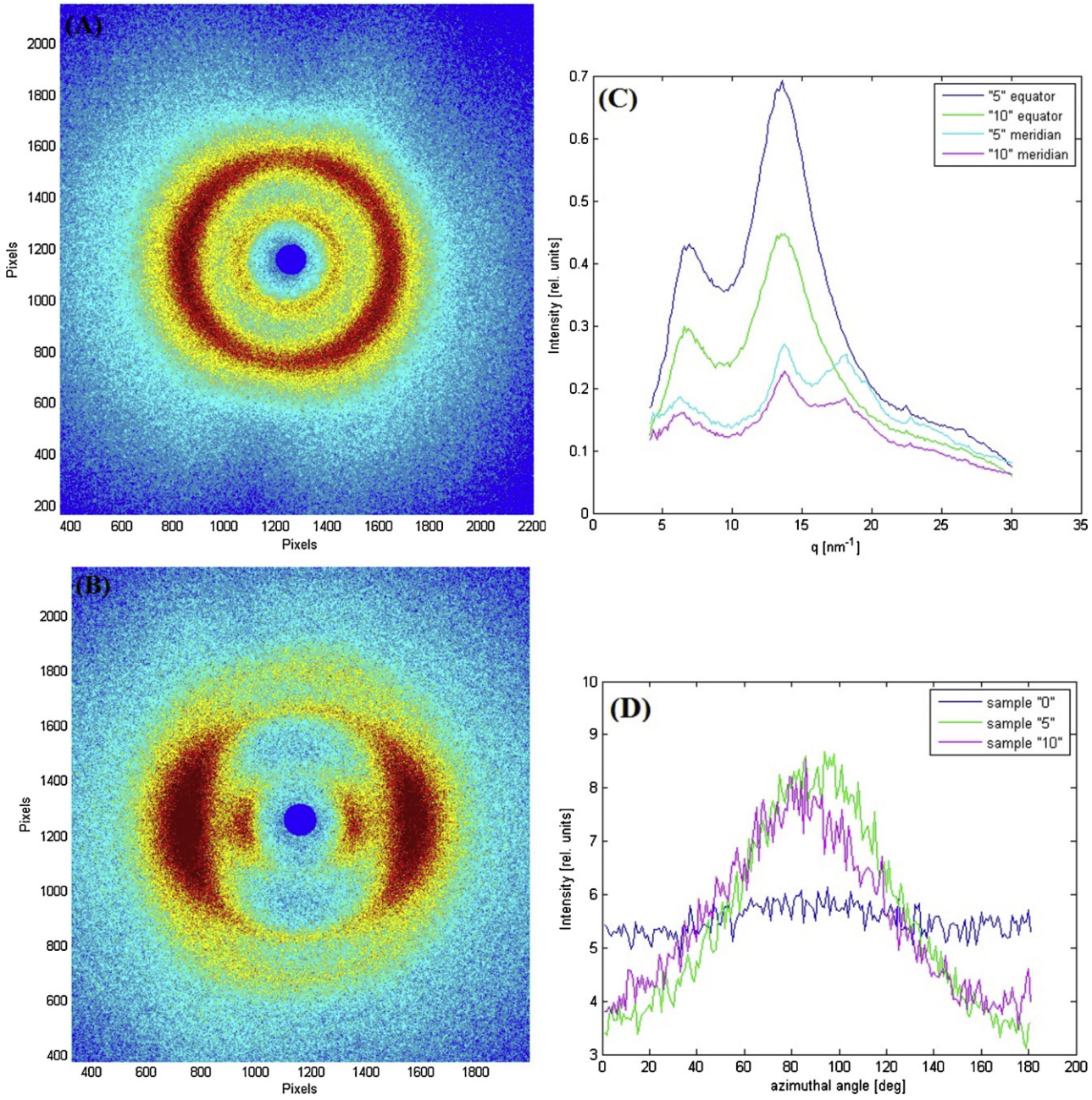

Fig. 7. 2D-SWAXS of (a) pure hyaluronan fibers mounted vertically (a little of axis). Its orientation can be seen from the slight difference between the meridian and equatorial reflections. (b) Hyaluronan fibers incorporated in silver nanoparticles (5 mM) mounted vertically (a little of axis). Here the difference between meridian and equatorial reflections is clearly enhanced. (c) Comparison of meridian and equatorial reflections of fibers (5 mM and 10 mM). The little peaks at $q = 22.253\ nm^{-1}$ and $q = 26.82\ nm^{-1}$ correspond to the [1 1 0] and [1 1 1] peaks of Ag which are also seen by powder diffraction and discussed in the appropriate section. (d) Comparison of normalized azimuth profiles of the first strong reflection for samples pure hyaluronan fiber, hyaluronic treated with (5 mM and 10 mM) of silver nitrate. Treatment by silver nanoparticles apparently increases orientation.

Please cite this article in press as: Abdel-Mohsen, A. M., et al. Green synthesis of hyaluronan fibers with silver nanoparticles. *Carbohydrate Polymers* (2012), doi:10.1016/j.carbpol.2012.03.022

prepared by wet spinning technique and there can be seen, the prepared fiber has a smooth and homogenous structure. The same conclusion can be done for the fibers with incorporated in different concentrations of silver nanoparticles (Fig. 6C-b–e).

3.2.6. Effect of concentration of silver nanoparticles on the mechanical properties of hyaluronic fibers

Table 1 shows the mechanical properties of hyaluronane fibers with different quantity of Ag^0 nanoparticles. From the obtained data, it can be concluded, that all prepared fibers can be used for the fabrication of textile materials by classical textile techniques (woven or non-woven textiles).

3.2.7. Two-dimensional X-ray scattering (2D SWAXS)

Fig. 7 shows the (2D SWAXS) pattern of hyaluronan fibers and fibers with silver nanoparticles.

The fibers were measured using SWAXS camera Molmet. Its feasibility for this purpose had been tested measuring a commercial fiber. First 2D SAXS detector was used probing the region $q = (0.5–10)\ nm^{-1}$ (see Section 2.3.6). This gave not much useful information. Therefore the imaging plate (IP) was employed and its distance from the sample was optimized to circa 0.2 m. Thereby 2D images probing the range $q = (4–30)\ nm^{-1}$ were obtained. They match the SAXS data on their low q side, powder diffraction data $q = (7.11–52.45\ nm^{-1})$ (see Section 3.2.5) on their high q side and contain the most interesting information obtainable by X-Ray scattering. Further we deal only with the IP data but the both probed regions could be used, e.g. to fit a structural model.

Here we shows our technique applied on three samples: pure hyaluronan fiber and two fibers with different concentrations of silver nitrate 5 mM and 10 mM, denoted as "0", "5" and "10" respectively.

The scattering image of the pure hyaluronic fibers Fig. 7-A shows not measurable crystallinity and very poor orientation, judged only from slight asymmetry between meridian and equatorial reflections. The scattering image of hyaluronan fiber (10 mM) Fig. 7-B shows that adding AgNPs might have improved crystallinity, which is still impossible to see and evaluate but orientation has apparently increased considerably.

The extremely poor quality of scattering does not allow reliable indexing and building of a reasonable model and thus to interpret the changes caused by adding silver precisely on the basis of a structural model. The orientation can be estimated from the difference of the equatorial and meridian profiles in Fig. 7-C. It seems likely that adding Ag improves orientation but increasing twice the Ag concentration from 5 mM to 10 mM does not make much change. To evaluate orientation more precisely we have used azimuthal profiles in the region of the first maxima $q = 0.665\ A^{-1}$ which is present in diffractograms of all three samples. Normalized azimuthal profiles are shown in Fig. 7-D. The profile of the untreated sample "0" clearly differs from the other two profiles of samples "5" and "10" with added Ag. To express this quantitatively we evaluate the width of each profile by its second central moment σ and estimate the orientation using a simple orientation factor $ofact = (90 - \sigma)/90$. This formula had been used in literature in similar cases of poor quality data. It gives 1 for fully oriented and 0 for fully unoriented samples. For the samples "0", "5" and "10" the σ is 51, 45 and 47 and ofact is 0.43, 0.48 and 0.49 respectively. Our orientation factor is not very sensitive and for instance does not sufficiently numerically illustrate the difference clearly visible in Fig. 7. However, on its basis we can anyway make the following conclusions:

1) Even the untreated sample "0" is slightly oriented
2) Adding Ag nanoparticles improves the orientation but there is no significant difference even when doubling the concentration from 5 mM to 10 mM.

4. Conclusion

Environmentally and "green approach" to the preparation of silver nanoparticles by using hyaluronan fibers, hyaluronan fiber acted as a reducing agent and stabilizer for the formed AgNPs. The use of environmentally friendly materials (hyaluronan fiber) offers numerous benefits ranging from environmental friendliness to readiness for an integration of these nanomaterials to biologically relevant systems. The preparation of the nanoparticles relied on a concentration of hyaluronan fibers as well as silver nitrate concentration in addition to pH, temperature and duration of the reduction reaction. The hyaluronan fiber was prepared by dissolved it in slightly alkaline solution of sodium hydroxide and spinning the aging solution by wet spinning technique using mixture of acetic/methanol in a coagulation bath. (TEM), XRD, UV/Vis spectroscopy, (ICP OES), (2D SWAXS), and (SEM) confirmed AgNPs, The so obtained AgNPs incorporated into hyaluronan fibers were stable and remained without aggregation for more than 90 days. The mechanical properties of hyaluronan fibers were measured after and before incorporated into silver nanoparticles. This methodology can also be adapted to the preparation of other metal nanoparticles. The preliminarily results of silver nanoparticles incorporated in hyaluronan fibers showed high biological activity. AgNPs incorporated in the hyaluronan fibers can be used in the different biomedical purposes especially in wound healing and dressing purposes.

Acknowledgement

This work was supported by research grant VZ MSMT 0021627502, Czech Republic and VZ MSMT 0021627501.

References

Abdel-Mohsen, A. M., Aly. A. S., & Hrdina, R. (2012). A novel method for the preparation of silver/chitosan-O-methoxy polyethylene glycol core shell nanoparticles. Journal of Polymers and the Environment, doi:10.1007/s10924-011-0378, in press. http://www.springerlink.com/content/j35n6374v2315644/fulltext.pdf.

Alkrad, J. A., Mrestani, Y., Stroehl, D., Wartewig, S., & Neubert, R. (2003). Characterization of enzymatically digested hyaluronic acid using NMR, Raman, IR, and UV-Vis spectroscopes. *Journal of Pharmaceutical and Biomedical Analysis*, *31*, 545–550.

Bohren, C. F., & Huffman, D. R. (1998). *Absorption and scattering of light by small particles*. New York: John Wiley & Sons Inc., pp. 210–231

Burgert, L., Hrdina, R., Mašek, D., & Velebný, V. (2010). Fibers from hyaluronan, their preparation and application. CZ patent application 2010-1001. CPN spol. s r.o. Dolní Dobrouč, Czech Republic.

Chang, C., You Apiwat, C., & Vincent, M. R. (2007). The biomacromolecule–nanoparticle interface. *Nanotoday*, *2*, 34–43.

Chen, J. Y., Chen, D. L., Wang, J. F., Xi L. m Au, A., Siekkinen, A., & Warsen, M. (2007). Immune gold nanocages with tailored optical properties for targeted photothermal destruction of cancer cells. *Nano Letters*, *7*, 1318–1322.

Dash, M., Chiellini, F., Ottenbrite, R. M., & Chiellini, E. (2011). Chitosan-A versatile semi-synthetic polymer in biomedical applications. *Progress in Polymer Science*, *26*, 981–1014.

Du, W. L., Du, S. S., Niu, Y. L., Xu, Z. R., & Fan, C. L. (2009). Antibacterial activity of chitosan tripolyphosphate nanoparticles loaded with various metal ions. *Carbohydrate Polymers*, *75*, 385–389.

Eriksson, S., Fraser, J. R. E., Laurent, T. C., Pertoft, H., & Smedsrod, B. (1983). Endothelial cells are a site of uptake and degradation of hyaluronic acid in the liver. *Experimental Cell Research*, *144*, 223–228.

Gao, S. Y., Zhang, H. J., Wang, X. M., Yang, J. H., Zhou, L., Peng, C. Y., et al. (2005). Unique gold sponges: Biopolymer-assisted hydrothermal synthesis and potential application as surface-enhanced Raman scattering substrates. *Nanotechnology*, *16*, 2530–2535.

Han, M. Y., Quek, C. H., & Huang, W. (1999). A simple and effective chemical route for the preparation of uniform non-aqueous gold colloids. *Chemical Material*, *11*, 1144–1147.

Henglein, A., & Giersig, M. (2000). Reduction of Pt (II) by H_2: Effects of citrate and NaOH and reaction mechanism. *Journal of Physical Chemistry B*, *104*, 6767–6772.

Hideki, S., Kanda, T., Shibata, H., Ohkubo, T., & Abe, M. (2006). Preparation of highly dispersed core/shell-type titania nanocapsules containing a single Ag nanoparticle. *Journal of American Chemical Society*, *128*, 4944–4945.

Ji, M., Chen, X., Wai, C. M., & Fulton, J. L. (1999). Synthesizing and dispersing silver nanoparticles in a water-in-supercritical carbon dioxide microemulsion. *Journal of American Chemical Society*, *121*, 2631–2632.

Jradi, S., Balan, L., Zeng, X. H., Plain, J., Lougnot, D. J., & Royer, P. (2010). Spatially controlled synthesis of silver nanoparticles and nanowires by photosensitized reduction. *Nanotechnology*, *21*, 95605–95612.

Kvitek, L., Prucek, R., Panacek, A., Novotny, R., Hrbac, J., & Zboril, R. (2005). The influence of complexing agent concentration on particle size in the process of SERS active silver colloid synthesis. *Journal of Material Chemistry*, *15*, 1099–1105.

Lapcik, L., Smedt, D., Demeester, S., & Chabrecek, J. P. (1998). Hyaluronan: Preparation, structure, properties, and applications. *Chemical Review*, *98*, 2663–2684.

Lim, B., Jiang, M., & Yu, T. (2010). Nucleation and growth mechanisms for Pd–Pt bimetallic nanodendrites and their electrocatalytic properties. *Nano Research*, *3*, 69–80.

Lubomir, L., Jr., Stefan, D. S., Joseph, D., & Peter, C. (1998). Hyaluronan: Preparation, structure, properties, and applications. *Chemical Review*, *98*, 2663–2684.

Mayer, A. B. R., Grebner, W., & Wannemacher, R. (2000). Preparation of silver–latex composites. *Journal of Physical Chemistry B*, *104*, 7278–7285.

Muzzarelli, R. A. A. (2011). Chitosan composites with inorganics, morphogenetic proteins and stem cells, for bone regeneration. *Carbohydrate Polymers*, *83*, 1433–1445.

Nogueira, H. I. S., Soares, C. R., Cruz, S. G., & Trindade, T. (2002). Adsorption of 2,2-dithiodipyridine as a tool for the assembly of silver nanoparticles. *Journal of Material Chemistry*, *12*, 2339–2342.

Pastoriza, S. I., & Liz, L. M. (1999). Formation and stabilization of silver nanoparticles through reduction by *N*,*N*-dimethyl formamide. *Langmuir*, *15*, 948–951.

Pathak, S., Greci, M. T., & Kwong, R. C. (2000). Synthesis and applications of palladium-coated poly (vinyl pyridine) nanospheres. *Chemical Material*, *12*, 1985–1989.

Raveendran, P., Fu, J., & Wallen, S. L. (2003). Completely green synthesis and stabilization of metal nanoparticles. *American Chemical Society*, *125*, 13940–13941.

Raveendran, P., Fu, J., & Wallen, S. L. (2006). A simple and green method for the synthesis of Au, Ag, and Au–Ag alloy nanoparticles. *Green Chemistry*, *8*, 34–38.

Reineck, I., DeAnna, J., Suleski, T. J., Lee, S. A., & Rupprecht, A. (2003). A Raman study of the hydration of wet-spun films of Li-hyaluronate. *Journal of Bimolecular Structure and dynamics*, *21*, 153–157.

Shah, P. S., Holmes, J. D., Doty, R. C., Johnston, K. P., & Korgel, B. A. (2000). Steric stabilization of nanocrystals in supercritical CO_2 using fluorinated ligands. *Journal of American Chemical Society*, *122*, 4245–4246.

Shameli, K., Ahmad, M. B., & Yunus, W. (2010). Silver/poly (lactic acid) nanocomposites: Preparation, characterization, and antibacterial activity. *International Journal of Nanomedicine*, *5*, 573–579.

Shen, J., Shi, M., & Li, N. (2010). Facile synthesis and application of Ag-chemically converted graphene nanocomposites. *Nano Research*, *3*, 339–349.

Sheng, Li., Yangyang, Z., xiaojuan, Xu., & Lina, Z. (2011). Triple helical polysaccharide induced good dispersion of silver nanoparticles in water. *Biomacromolecules*, *12*, 2864–2871.

Steffan, M., Steffan, A., Jakob, P., & Lang, H. (2009). Silica supported silver nanoparticles from a silver (I) carboxylate: Highly active catalyst for regioselective hydrogenation. *Catalysis Communications*, *10*, 437–441.

Sun, Y., Yin, Y., Mayers, B. T., Herricks, T., & Xia, Y. N. (2002). Uniform silver nanowires synthesis by reducing $AgNO_3$ with ethylene glycol in the presence of seeds and poly (vinyl pyrrolidone). *Chemistry of Materials*, *14*, 4736–4745.

Tan, Y., Li, Y., & Zhu, D. (2003). Preparation of silver nanocrystals in the presence of aniline. *Journal of Colloid and Interface Science*, *258*, 244–251.

Tao, A., Kim, F., Hess, C., Goldberger, J., He, R. R., Sun, Y. G., et al. (2003). Silver nanowire monolayers for molecular sensing using surface-enhanced Raman spectroscopy. *Nano Letter*, *3*, 1229–1233.

Templeton, A. C., Chen, S., Cross, S. M., & Murray, R. W. (1999). Water-soluble, isolable gold clusters protected by tiopronin and coenzyme A monolayers. *Langmuir*, *15*, 66–76.

Torigoe, K., Suzuki, A., & Esumi, K. (2001). Au (III)–PAMAM interaction and formation of Au–PAMAM nanocomposites in ethyl acetate. *Journal of Colloid Interface Science*, *241*, 346–356.

Underhillm, R. S., & Liu, G. (2000). Preparation and performance of Pd particles encapsulated in block copolymer nanospheres as a hydrogenation catalyst. *Chemical Material*, *12*, 3633–3641.

Van, H., Klemperer, D. L., Wo, G., & Zukoski, C. F. (2001). Characterization of colloidal stability during precipitation reactions. *Langmuir*, *17*, 3120–3127.

Vigneshwaran, N., Nachane, R. P., Balasubramanya, R. H., & Varadarajan, P. V. (2006). A novel one-pot green synthesis of stable silver nanoparticles using soluble starch. *Carbohydrate Research*, *341*, 2012–2018.

Wan, A., Sun, Y., Li, G., & Li, H. L. (2009). Preparation of aspirin and probucol in combination loaded chitosan nanoparticles and in vitro release study. *Carbohydrate Polymers*, *75*, 566–574.

Wang, J., Neoh, K. G., & Kang, E. T. (2001). Preparation of nanosized metallic particles in polyaniline. *J Colloid and Interface Science*, *239*, 78–86.

Wang, Y., Ren, J., & Deng, K. (2000). Preparation of tractable platinum, rhodium, and ruthenium nanoclusters with small particle size in organic media. *Chemical Material*, *12*, 1622–1627.

Wu, M. L., Chen, D. H., & Huang, T. C. (2001). Evidence for seed-mediated nucleation in the chemical reduction of gold salts to gold nanoparticles. *Chemical Material*, *13*, 2313–2322.

Yin, Y., Li, Z. Y., & Zhong, Z. (2002). Synthesis and characterization of stable aqueous dispersions of silver nanoparticles through the Tollens process. *Journal of Material Chemistry*, *12*, 522–527.

Please cite this article in press as: Abdel-Mohsen, A. M., et al. Green synthesis of hyaluronan fibers with silver nanoparticles. *Carbohydrate Polymers* (2012), doi:10.1016/j.carbpol.2012.03.022